Theoretical Studies of the Tautomers of Pyridinethiones

Yu Adam Zhang, Vishakha Monga, Chris Orvig,* and Yan Alexander Wang*

Department of Chemistry, University of British Columbia, Vancouver, BC V6T 1Z1, Canada

Received: June 7, 2007; In Final Form: October 29, 2007

Pyridinethiones are important ligand precursors of coordination complexes of therapeutic value. In aqueous solution, pyridinethiones can dimerize and tautomerize to the corresponding thiols. However, the tautomerism of pyridinethiones, which can impact on therapeutic performance, is yet not fully understood. To resolve this important issue, we have carried out ab initio and DFT calculations to compute the geometries, energies, dipole moments, and NMR, IR, and UV−vis spectroscopic properties of all possible tautomers of pyridinethiones and compared our theoretical results with the existing experimental data. We found that the thione form of the tautomer is dominant for monomers of the pyridinethiones studied here. This work can serve as a reference for exploring other similar organosulfur compounds.

Introduction

There has been continued interest in organosulfur compounds with thiocarbonyl groups because of their diverse chemistry,[1] various biological applications,[2,3] and the tendency of the C═S bond to oxidize easily to form the corresponding thiols and disulfides.[4] Pyranthiones and pyridinethiones are two important classes of such organosulfur compounds.[5] Four years ago, pyranthiones were explored as ligands because of their trans-influencing ability.[6] A number of pyridinethiones have also been patented for their therapeutic antioxidant properties[7] and effectiveness against carcinoma.[8]

Pyridinethiones and their oxygen analogues, pyridinones, can tautomerize to the corresponding thiol/enol form (Figure 1).[9,10] It has been shown, however, that the prevailing form of these compounds is the thione/ketone form.[11] For pyridinethiones, the S−H group in the thiol form can easily oxidize to bridge two molecules through a disulfide bond in polar solvents in air (Scheme 1).[10,12] Interestingly, Stoyanov et al. reported that pyridinethiones convert to the thiol tautomer when left in aqueous or alcoholic solutions for ∼24 h, even though the thione form is more dominant.[10] Evidence for this tautomerism was also observed recently in the syntheses of pyridinethiones studied by our group.[5]

We recently reported[5] the preparation of 3-hydroxy-2-methyl-4-*p*-pyridinethione (Hmppt) and 3-hydroxy-1,2-dimethyl-4-*p*-pyridinethione (Hdppt) by reacting thiomaltol with ammonia and methylamine (Scheme 2), respectively. The resulting pyridinethiones were thoroughly characterized by elemental analysis, electron impact mass spectrometry, melting point determination, as well as UV-visible absorption, IR, and NMR spectra. X-ray crystal structures were also obtained for some of these compounds. Although the thiol and thione forms of the tautomer could not be separately isolated, some experimental characterization data suggested that the thione form is the dominant tautomer. A strong $\nu_{C=S}$ stretch in the IR spectra confirmed the thione form of the tautomer to be the solid-state chemical structure of the pyridinethiones. The solution-state characterization (via NMR and UV−vis spectra) of these compounds also suggests the presence of the thione tautomeric forms. Nonetheless, the data collected could not be unambiguously assigned to one tautomeric form over the other.

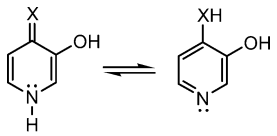

X=O; pyridinones
X=S; pyridinethiones

Figure 1. Tautomeric forms of pyridinones and pyridinethiones.

TABLE 1: Selected Bond Lengths (in Å) and Bond Angles (in deg) of Hdppt Dimer

bond	X-ray[a]/theory[b]	bond angles	X-ray[a]/theory[b]
S(1)−S(1*)	2.0472(7)/2.1306	S(1)−S(1*)−C(1)	104.22(5)/102.59
S(1)−C(1)	1.763(1)/1.771	S(1)−C(1)−C(2)	112.1(1)/119.8
O(1)−C(2)	1.278(2)/1.245	S(1)−C(1)−C(5)	126.0(1)/119.3
N(1)−C(3)	1.362(2)/1.355	C(3)−N(1)−C(4)	123.0(1)/122.8
N(1)−C(4)	1.351(2)/1.364	C(3)−N(1)−C(7)	119.4(1)/119.3
N(1)−C(7)	1.482(2)/1.472	C(4)−N(1)−C(7)	117.5(1)/117.9
C(1)−C(2)	1.424(2)/1.457	N(1)−C(3)−C(2)	119.9(1)/121.2
C(1)−C(5)	1.383(2)/1.390	N(1)−C(3)−C(6)	120.1(1)/120.7
C(2)−C(3)	1.427(2)/1.462	N(1)−C(4)−C(5)	119.9(1)/119.4
C(4)−C(5)	1.377(2)/1.385	O(1)−C(2)−C(1)	120.8(1)/124.4
C(3)−C(6)	1.489(2)/1.497	O(1)−C(2)−C(3)	123.4(1)/121.0
		C(2)−C(1)−C(5)	121.9(1)/120.6
		C(1)−C(2)−C(3)	115.8(1)/114.6
		C(1)−C(5)−C(4)	119.4(1)/121.3
		C(2)−C(3)−C(6)	120.0(1)/118.1

[a] From ref 5a, with experimental uncertainty shown in the parentheses. [b] Optimized geometry from B3LYP/6-31G(d,p) calculations.

As mentioned before, when left in aqueous or alcoholic solutions, the monomeric (thiol) forms of these compounds were found to convert to their dimeric (disulfide) forms. Evidence for the formation of an S−S bridge between two molecules was obtained with IR and NMR spectra. Unfortunately, the S−H or N−H proton could not be assigned distinctly due to probable exchange of the proton between S and N in solution (Figure 1). This process has been studied before, and the structures have been verified by comparing the experimental data with theoretical calculations for the IR and NMR data.[10] Hence, more extensive comparisons between the theoretical and experimental

* Corresponding authors. Phone: 1-604-222-3799; Fax: 1-604-822-2847. E-mail: yawang@chem.ubc.ca (Y.A.W.).

10.1021/jp0744026 CCC: $40.75
Published on Web 03/15/2008

SCHEME 1. Proposed Mechanism for the Dimerization of the Two Pyridinethiones Studied in this Work: 3-Hydroxy-2-methyl-4-*p*-pyridinethione (Hmppt) and 3-Hydroxy-1,2-dimethyl-4-*p*-pyridinethione (Hdppt)

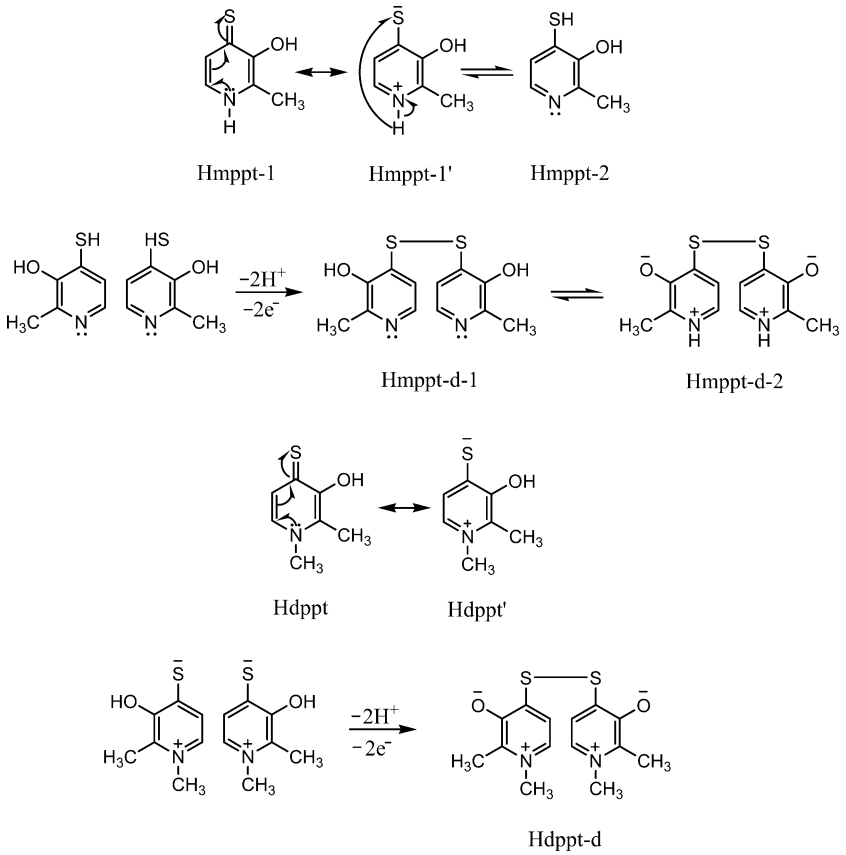

SCHEME 2. Synthesis of the Pyridinethiones[a]

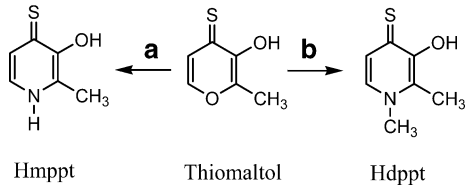

[a] (a) excess NH_4OH, H_2O/EtOH, 34 °C, 36 h; (b) excess 40% $MeNH_2$, H_2O, 75 °C, 12 h.

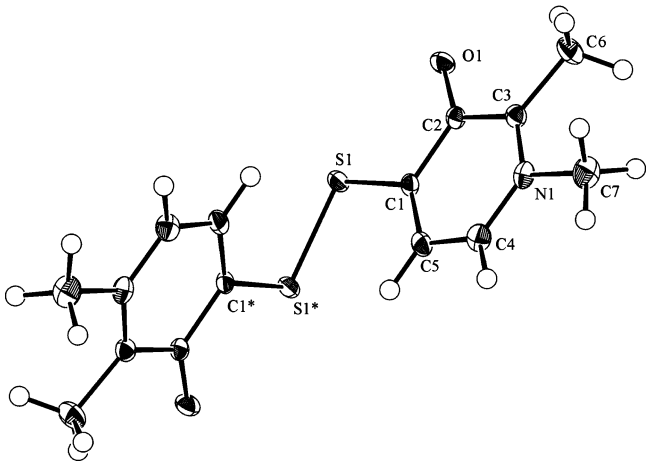

Figure 2. ORTEP diagram of Hdppt dimer (50% thermal ellipsoids), adapted from ref 5a.

data should allow the assignment of the dominant tautomeric form of these pyridinethiones.

Herein, we report ab initio and DFT calculations of Hmppt, its methyl analog (Hdppt), their thiol tautomers, and their dimeric forms. Our results reported here provide a comprehensive library of data for any future comparisons of these and other such similar compounds.

TABLE 2: Theoretical Predictions of the Dipole Moments (in D) of All Tautomers in Different Media (vacuum, DMSO, or H_2O), Calculated at the B3LYP/6-311++G(2df,p)// B3LYP/6-31G(d,p) Level of Theory

tautomer	vacuum	DMSO	H_2O
Hmppt-1	7.53	12.64	12.74
Hmppt-2	2.18	3.54	3.72
Hmppt-d-1	1.67	3.62	3.83
Hmppt-d-2	10.06	18.84	19.38

Details of Computational Methods

We have performed ab initio and DFT calculations to obtain the NMR, IR, and UV−vis data for Hmppt, Hdppt, and their dimers. We optimized Hmppt-1 and Hmppt-2 in the gas phase at the B3LYP[13]/6-31G(d,p) and B3LYP/6-311++G(2df,p) levels of theory and found only negligible differences between the two types of geometries. So we will use the B3LYP/6-31G(d,p) geometries for all species throughout this paper, unless specially mentioned. Geometries of Hmppt-1 and Hmppt-2 obtained on different levels are included in the Supporting Information for reference. The total energies and the Gibbs free energies (at 298 K) of molecules of interest were computed at the B3LYP/6-31G(d,p) and MP2/6-31G(d,p) levels of theory. Partial charges were computed from the natural bond orbital (NBO) analysis.[14] The ^{13}C and ^{1}H NMR chemical shifts of all tautomers were predicted with the gauge-independent atomic orbital (GIAO)[15] and the continuous set of gauge transformations (CSGT)[16] approaches at the HF/6-311++G(2df,p), MP2/6-311++G(2df,p), B3LYP/6-311++G(2df,p), and PBEPBE/6-

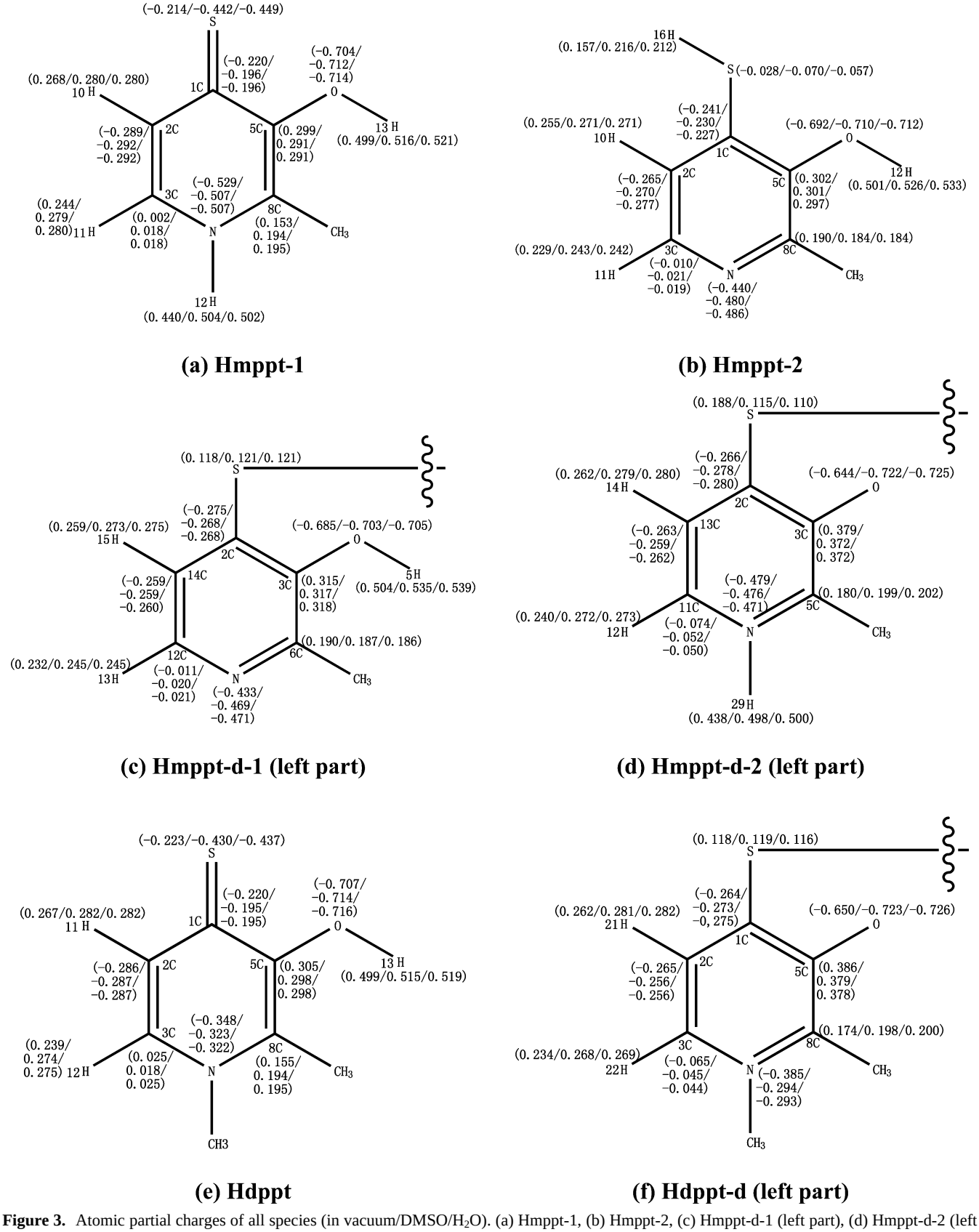

Figure 3. Atomic partial charges of all species (in vacuum/DMSO/H_2O). (a) Hmppt-1, (b) Hmppt-2, (c) Hmppt-d-1 (left part), (d) Hmppt-d-2 (left part), (e) Hdppt, (f) Hdppt-d (left part).

311++G(2df,p) levels of theory. The polarizable continuum model[17] (PCM) was employed to account for the solvation effects. All geometries were reoptimized at the B3LYP/6-31G-(d,p) level in the solution environment. Vibrational frequencies were calculated at the HF, MP2, and B3LYP levels of theory with the basis set 6-31G(d,p). To improve the agreement between theory and experiment, we took the usual practice of employing scaling factors to bring our calculated frequencies closer to the existing experimental data.[18] Since the scaling factor for B3LYP/6-31G(d,p) calculations is not available, we instead

TABLE 3: Total Energy and Gibbs Free Energy (at 298 K) Differences with the Zero-Point Energy Correction (in kcal/mol) of All Tautomers in Different Media (vacuum, DMSO, or H_2O), Calculated at the B3LYP/6-31G(d,p) and MP2/6-31G(d,p)// B3LYP/6-31G(d,p) Levels of Theory

		vacuum		DMSO		H_2O	
energy difference	method	ΔE	ΔG	ΔE	ΔG	ΔE	ΔG
$E_{\text{Hmppt-2}} - E_{\text{Hmppt-1}}$	B3LYP	4.0	4.1	12.5	12.3	12.6	12.1
	MP2	−0.3	−0.9	7.9	7.7	7.9	7.6
$E_{\text{Hmppt-d-2}} - E_{\text{Hmppt-d-1}}$	B3LYP	26.6	26.4	5.2	5.3	4.4	4.0
	MP2	27.8	27.6	8.0	8.0	7.5	7.1

TABLE 4: Theoretical IR Peak Positions (in cm^{-1}) and Intensities of the Important Peaks (in parentheses) Calculated at the HF/6-31G(d,p), MP2/6-31G(d,p), and B3LYP/6-31G(d,p) Levels of Theory, Compared with the Experimental Results

	HF	MP2	B3LYP	expt[a]	assignment[b]
scaling factor[c]	0.8992	0.9370	0.9614		
Hmppt-1	3055(171.5)	3161(98.0)	3192(160.4)	3061	ν_{NH} (ν_{OH})
				2932	ν_{NH} (ν_{OH})
				2821	ν_{NH} (ν_{OH})
	3329(182.5)	3455(177.0)	3499(119.5)	3427	ν_{OH} (ν_{NH})
	1605	1598	1607	1590	ring and C−N−C bands
	1442	1456	1414	1445	ring and C−N−C bands
	1189	1250	1220	1216	ring and C−N−C bands
	1136(468.5)	1154(119.1)	1162(104.9)	1174	$\nu_{C=S}$
	869	858	874	886	ring and C−N−C bands
	804	805	826	782	ring and C−N−C bands
Hmppt-2	3356(128.1)	3488(104.2)	3527(104.2)	3427	(ν_{OH})
	2437(5.9)	2507(4.1)	2553(9.1)		(ν_{SH})
	1577	1542	1561	1590	ring and C−N−C bands
	1470	1452	1431	1445	ring and C−N−C bands
	1226	1218	1208	1216	ring and C−N−C bands
	1157(12.9)	1124(53.5)	1134(55.9)	1174	(ν_{C-S})
	850	840	894	886	ring and C−N−C bands
	767	788	805	782	ring and C−N−C bands
Hmppt-d-1	3370(133.7)	3505(103.3)	3544(126.6)	3508	ν_{H2O} (ν_{OH})
	1574		1556	1630	ring and C−N−C bands
	1535	1534	1545	1510	ring and C−N−C bands
	1226	1218	1203	1215	ring and C−N−C bands
	849	839	851	833	ring and C−N−C bands
	798	789	803	816	ring and C−N−C bands
Hmppt-d-2	3285(165.7)	3398(115.9)	3437(93.6)	3417	(ν_{NH})
				2806	(ν_{NH})
				2731	(ν_{NH})
	1587	1655	1608	1630	ring and C−N−C bands
	1518	1530	1565	1510	ring and C−N−C bands
	1218	1227	1232	1215	ring and C−N−C bands
	856	840	858	833	ring and C−N−C bands
	817	802	818	816	ring and C−N−C bands

[a] See the Supporting Information of ref 5a (with a ±4 cm^{-1} uncertainty). [b] See ref 5a. New assignments from this work are shown in parentheses. [c] See ref 18.

used the scaling factor for B3LYP/6-31G(d), which should not bring any significant numerical error. Time-dependent density functional theory[19] (TDDFT) with different density functionals (B3LYP and PBEPBE[20]) was utilized to calculate the UV−vis spectra. All calculations were performed with the quantum chemistry package of Gaussian 03.[21]

Results and Discussions

Both Hmppt and Hdppt can dimerize in solution. While in solution, it is very difficult to crystallize the Hmppt monomer/dimer mixture, so X-ray data are available only for Hdppt dimer.[5a] X-ray-quality crystals for Hdppt dimer were obtained by slow evaporation in ethyl acetate. The structure is shown in Figure 2, and the selected bond lengths and bond angles are listed in Table 1. For comparison, we also provide the data of the optimized geometry from our DFT calculations.

As can be seen in Table 1, our theoretical results agree quite well with the experimental X-ray data. Because the S−S bond is very flexible, we imposed C_2 symmetry on the dimer to accelerate the calculation and to reduce the demand on computational resources (especially in the property calculations). In the end, we found that the optimized geometry without the C_2 symmetry constraint is virtually identical to that obtained with the constraint. Thus, it is legitimate for us to impose the same C_2 symmetry constraint in additional calculations whenever possible.

We carried out NBO partial charge analysis for Hmppt-1 and other molecules shown in Scheme 1 (Hmppt-1′ is a resonance form of Hmppt-1). The partial charge results are shown in Figure 3. For Hmppt-1, we found that both in vacuum and in solution (H_2O or DMSO), the N atom always carries a large negative charge (> -0.5), and the S atom always carries a relatively small negative charge (< -0.5). This might suggest that Hmppt-1′ poorly represents the actual electronic structure, since in Hmppt-1′ the N atom should carry less negative charge than usual and the S atom should carry more negative charge. Moreover, the bond length of C1−C2 (see the numbering in Figure 3) in Hmppt-1 is calculated to be 1.43 Å, which is much longer than the bond length of C2−C3 (1.37 Å), indicating a double bond structure between C2 and C3. Thus, it is safe to

TABLE 5: Theoretical ^{13}C and ^{1}H NMR Chemical Shifts (in ppm) of Hmppt-1 in DMSO, Calculated with the GIAO Method with the 6-311++G(2df,p) Basis Set at the HF, MP2, B3LYP, and PBEPBE Levels of Theory, Compared with Experimental Results Obtained in DMSO

	HF	MP2	B3LYP	PBEPBE	expt[c]
C1[a]	194.051	170.256	181.479	172.171	169.86
C2	129.948	137.288	134.273	131.980	125.22
C3	145.099	128.846	134.222	128.607	128.34
C5	154.951	163.986	161.364	158.655	151.76
C8	145.135	128.136	135.268	129.426	126.85
δ[b]	13.4	5.3	8.9	3.8	
H10	8.111	8.723	8.002	7.938	7.29
H11	8.399	7.733	7.767	7.598	7.50
H12	10.721	10.742	10.013	9.763	12.84
H13	8.137	8.026	8.162	8.181	8.64

[a] See Figure 2 for the numbering of the atoms. [b] Average absolute error with respect to the ^{13}C NMR experimental data. [c] From the Supporting Information of ref 5a.

TABLE 6: Theoretical ^{13}C and ^{1}H NMR Chemical Shifts (in ppm) of Hmppt-2 in DMSO, Calculated with the GIAO Method with the 6-311++G(2df,p) Basis Set at the HF, MP2, B3LYP, and PBEPBE Levels of Theory, Compared with Experimental Results Obtained in DMSO

	HF	MP2	B3LYP	PBEPBE	expt[c]
C1[a]	133.187	124.479	131.071	127.011	169.86
C2	134.987	134.989	136.307	133.869	125.22
C3	150.782	143.139	147.697	144.199	128.34
C5	158.595	160.767	161.260	158.135	151.76
C8	159.701	149.767	155.974	151.737	126.85
δ[b]	21.7		21.6	19.7	
H10	8.045	8.053	7.874	7.832	7.29
H11	8.651	8.414	8.434	8.407	7.50
H12	6.917	6.875	6.875	6.922	8.64
H16	5.340	5.246	4.903	4.881	12.84

[a] See Figure 2 for the numbering of the atoms. [b] Average absolute error with respect to the ^{13}C NMR experimental data. [c] From the Supporting Information of ref 5a.

TABLE 7: Theoretical ^{13}C and ^{1}H NMR Chemical Shifts (in ppm) of Hmppt-d-1 in DMSO, Calculated with the GIAO Method with the 6-311++G(2df,p) Basis Set at the HF, B3LYP, and PBEPBE Levels of Theory, Compared with Experimental Results Obtained in DMSO

	HF	B3LYP	PBEPBE	expt[c]
C2[a]	137.520	137.894	133.841	133.16
C3	158.745	159.879	156.344	148.99
C6	160.864	157.534	153.541	145.69
C12	149.800	147.231	143.949	139.25
C14	135.285	135.957	133.257	117.58
δ[b]	11.5	10.8	7.3	
H5	7.320	7.306	7.396	9.8
H13	8.588	8.382	8.371	7.87
H15	7.391	7.248	7.210	7.10

[a] See Figure 2 for the numbering of the atoms. [b] Average absolute error with respect to the ^{13}C NMR experimental data. [c] From the Supporting Information of ref 5a.

conclude that Hmppt-1′ does not represent the dominant form of the real electronic structure. We also found a similar situation in the charge and structural analyses of Hdppt and Hdppt′: Hdppt′ is not a good representation of the actual electronic structure of Hdppt.

Hdppt dimer might be somewhat different, since it can only exist in the formally charged form (see Scheme 1). Its N atom has a charge of ca. −0.3, smaller than those in Hmppt-1 and Hmppt-2 and their dimers, whereas its O atom carries a larger negative charge (> −0.7). These results, compared to charge distributions of Hmppt dimers, support the N-formal-positive-charged structure of Hdppt dimer, in agreement with the X-ray crystal structure data. It was also observed that different solvents affect the charge distributions slightly.

TABLE 8: Theoretical ^{13}C and ^{1}H NMR Chemical Shifts (in ppm) of Hmppt-d-2 in DMSO, Calculated with the GIAO Method with the 6-311++G(2df,p) Basis Set at the HF, B3LYP, and PBEPBE Levels of Theory, Compared with Experimental Results Obtained in DMSO

	HF	B3LYP	PBEPBE	expt[c]
C2[a]	144.950	149.495	146.440	133.16
C3	178.877	174.873	170.277	148.99
C5	159.927	153.375	147.689	145.69
C11	122.985	120.534	116.410	139.25
C13	138.287	136.011	133.203	117.58
δ[b]	18.6	17.4	15.0	
H12	7.637	7.318	7.158	7.87
H14	8.010	7.764	7.757	7.10
H29	12.192	11.256	10.943	9.8

[a] See Figure 2 for the numbering of the atoms. [b] Average absolute error with respect to the ^{13}C NMR experimental data. [c] From the Supporting Information of ref 5a.

The dipole moments of each species and total/free energy differences between them were also studied with small and large basis sets, both in vacuum and in solution (see Tables 2 and 3 and Supporting Information for details). We found that the basis set affects dipole moments only slightly. Dipole moments calculated from the small basis set are included in Supporting Information for reference. Data shown in Table 3 clearly indicate that Hmppt-1 is more stable than is Hmppt-2 in DMSO or H_2O, although the MP2 calculations predict that Hmppt-2 is just slightly more stable than is Hmppt-1 in vacuum. Such irregularity should not pose any real problem, because we already have coherent results (from different methods) for the relative stability in DMSO or H_2O, based on which we can compare our theoretical results with experimental data. As expected from those positive energy differences in Table 3, the more polar thione form of Hmppt is favored in the polar solution environment. In addition, the polar solvents even increase the energy difference between Hmppt-2 and Hmppt-1.

The dimers show another story. In the tautomerism of Hmppt, the proton migrates between the N and S atoms, but the proton migrates between the N and O atoms in Hmppt dimer. Hmppt-d-2 has a structure with a formal discrete positive/negative charge distribution that usually has an higher energy in vacuum, and its dipole moment is very large (∼10 D), compared to the small dipole moment of Hmppt-d-1 (only ∼1.7 D in vacuum). Although Hmppt-d-1 is favored in terms of total energy, the energy difference between Hmppt-d-2 and Hmppt-d-1 is smaller than the corresponding values of the Hmppt monomeric tautomers in solutions. This is, of course, because polar solvents can stabilize the more polar Hmppt-d-2.

It is interesting to consider how the S and H atoms are bonded in these molecules, so we carried out vibrational frequency calculations and compared the results with the experimental data. The final results are shown in Table 4. Experimental IR data were collected from samples in solid phase, but a broad ν_{OH} peak for H_2O was seen in the IR spectrum of Hmppt dimer because the sample was not dry. In addition, O−H groups in Hmppt or in H_2O can form H-bonds with other O−H and N−H groups, which makes the IR spectrum above 2700 cm^{-1} very complicated. Hence, it is very difficult to match the calculated results with the experimental data precisely. Theoretically, we found that the vibrational frequencies of O−H and N−H bonds are 3055−3192 and 3329−3499 cm^{-1}, respectively, in direct contradiction to previous experimental assignments:[5a] 3427 cm^{-1}

TABLE 9: Theoretical UV−vis Absorption Positions (in nm) and Oscillator Strengths (in Parentheses) for Single Excitations of Thiol and Thione Tautomers of Hmppt and Hmppt Dimer in Vacuum and H_2O, Calculated at B3LYP Levels, Compared with Experimental Data Obtained in H_2O[e]

tautomers	vacuum	H_2O	expt[a]	tautomers	vacuum	H_2O	expt[a]
Hmppt-1[c]	206 (0.2072)	206 (0.2621)	210 (4.13)	Hmppt-d-1[d]	270 (0.2546)	264 (0.2938)	270 (3.71)
	H[b]−3 → L[b] 0.29	H−3 → L −0.23			H−5 → L 0.67	H−5 → L 0.67	
	H−2 → L+2 0.53	H−2 → L+1 0.56			323 (0.0002)	323 (0.0029)	336 (4.32)
	H−1 → L+6 −0.14	H−1 → L+4 −0.14			H−5 → L 0.10	H−4 → L −0.13	
	H−1 → L+7 −0.21	H → L+6 0.19			H−2 → L 0.68	H−3 → L 0.65	
		H → L+10 0.11				H → L 0.12	
	252 (0.0975)	249 (0.1454)	245 (3.92)		364 (0.1262)	354 (0.1581)	
	H−2 → L 0.63	H−3 → L+1 0.13			H → L 0.68	H−3 → L −0.11	
	H−3 → L+2 −0.11	H−2 → L 0.61				H → L 0.67	
		H → L+1 0.19		Hmppt-d-2[d]	201 (0.2213)	203 (0.3136)	
	281 (0.0037)	280 (0.0001)	276 (3.43)		H−10 → L −0.14	H−10 → L −0.12	
	H−1 → L+1 0.70	H−2 → L −0.22			H−9 → L 0.11	H−7 → L 0.11	
		H → L+1 0.65			H−7 → L 0.19	H−6 → L+1 0.49	
	325 (0.3166)	319 (0.3693)	326 (4.21)		H−6 → L+1 0.33	H−5 → L+3 −0.10	
	H−2 → L+2 −0.12	H−2 → L+1 0.11			H−5 → L+4 −0.13	H−4 → L+4 −0.24	
	H → L 0.60	H → L 0.63			H−4 → L+3 0.13	H−3 → L+3 −0.16	
Hmppt-2[c]	199 (0.2005)	208 (0.0583)			H−3 → L+3 0.11	H−2 → L+4 −0.11	
	H−3 → L 0.41	H−3 → L −0.16			H−3 → L+5 −0.24	H−1 → L+4 −0.17	
	H−3 → L+1 −0.27	H−2 → L+1 −0.14			H−2 → L+6 0.32	H → L+3 0.13	
	H−2 → L+2 −0.15	H−1 → L+1 0.37			H−1 → L+3 −0.12		
	H−2 → L+3 0.11	H−1 → L+2 0.42			H → L+4 0.13		
	H−1 → L+3 0.15	H → L+1 0.12			220 (0.1801)	221 (0.1271)	
	H → L+1 −0.11	H → L+4 −0.27			H−7 → L+1 −0.12	H−6 → L 0.11	
	H → L+2 0.25				H−6 → L 0.23	H−5 → L+2 0.62	
	H → L+5 0.18				H−5 → L+2 −0.29	H−3 → L+4 −0.14	
	208 (0.0038)				H−4 → L+4 −0.22	H−1 → L+3 0.11	
	H−2 → L+1 0.27				H−3 → L+4 0.32		
	H−1 → L+1 0.55				H−2 → L+3 −0.26	228 (0.1235)	
	H−1 → L+2 0.26				H−1 → L+4 −0.11	H−7 → L+1 −0.15	
	H−1 → L+3 −0.12				H−1 → L+6 0.18	H−6 → L 0.21	
	239 (0.0013)	245 (0.0290)			H → L+3 0.12	H−5 → L+2 −0.23	
	H−3 → L −0.11	H−3 → L 0.11			H → L+5 −0.12	H−1 → L+3 0.49	
	H−2 → L 0.68	H−2 → L 0.49				H → L+5 −0.21	
		H−1 → L −0.42			234 (0.0777)		
		H → L+1 0.20			H−6 → L 0.48	234 (0.0257)	
	269 (0.0223)	266 (0.1388)			H−5 → L+2 0.19	H−4 → L+1 0.12	
	H → L +1 0.60	H−3 → L +1 0.12			H−4 → L+4 −0.13	H−4 → L+3 −0.10	
	H → L 0.30	H−2 → L −0.10			H−3 → L+4 −0.34	H−3 → L+2 0.42	
		H−1 → L+1 0.16			H−2 → L+3 0.14	H−3 → L+4 0.36	
		H → L 0.63			H → L+3 0.18	H−2 → L+3 −0.35	
Hmppt-d-1[d]	206 (0.0747)	206 (0.0426)	201 (4.27)		271 (0.0002)	269 (0.0008)	
	H−7 → L+1 0.19	H−7 → L+1 0.13			H−5 → L+1 0.65	H−2 → L+2 −0.12	
	H−5 → L+3 0.10	H−5 → L+3 0.10			H−1 → L+3 0.16	H−1 → L+2 0.67	
	H−3 → L+3 0.10	H−1 → L+2 0.24			H → L+4 −0.12		
	H−1 → L+2 0.30	H → L+3 −0.20			364 (0.1134)	318 (0.0844)	
	H → L+3 −0.25	H → L+4 0.53			H−3 → L+1 0.14	H−5 → L −0.19	
	H → L+4 0.42				H−1 → L+1 0.65	H−1 → L+1 0.63	
	H → L+6 −0.11				344 (0.0018)	337 (0.0005)	
	206 (0.0264)	206 (0.0279)			H−4 → L 0.29	H−4 → L 0.62	
	H−5 → L+1 −0.37	H−5 → L+1 −0.36			H−3 → L 0.21	H−3 → L+1 0.18	
	H−1 → L+3 −0.21	H−1 → L+3 −0.14			H−2 → L+1 −0.15	H → L+1 0.24	
	H−1 → L+4 0.49	H−1 → L+4 0.55			H−1 → L −0.14		
	H → L+2 0.13				H → L+1 0.47		
	245 (0.1157)	246 (0.1393)	238 (4.43)				
	H−7 → L+2 −0.11	H−7 → L+2 −0.12					
	H−5 → L+4 0.11	H−1 → L+1 0.66					
	H−1 → L+1 0.66						

[a] See the Supporting Information of ref 5a. [b] "H"and "L" denote the HOMO and the LUMO, respectively. "H−*m*" and "L+*n*" denote the *m*th orbital below the HOMO and the *n*th orbital above the LUMO, respectively. [c] Calculate at B3LYP/6-311++G(2df,p)//B3LYP/6-31G(d,p) level of theory. [d] Calculate at B3LYP/6-31G(d,p) level of theory. [e] Transitions with large CI coefficients are shown below each peak position.

for O−H and 3061 cm^{-1} for N−H vibrations. Even after we increased the basis set from 6-31G(d,p) to 6-311++G(2df,p) and reoptimized the geometries at B3LYP/6-311++G(2df,p), we still got 3179 cm^{-1} for O−H and 3484 cm^{-1} for N−H vibrations. Since all different theoretical methods employed here consistently predict the vibrational frequencies of O−H and N−H bonds, further computational studies employing more accurate (more computationally demanding and more time-consuming) ab initio methods should be carried out to fully resolve this discrepancy. Of course, an experimental revisit might also be necessary to settle this issue completely.

For the carbon−sulfur bond, the $\nu_{C=S}$ peak is observed in Hmppt but not in Hmppt dimer, which strongly suggests the formation of the S−S bond. Due to symmetry, we were unable to see the vibration of the S−S bond stretching in the IR spectra. It is clear that the calculated C═S stretching frequencies of Hmppt-1 agree better with the experimental data than do those of Hmppt-2 (the corresponding absolute average errors are 24

and 36 cm^{-1}, respectively), which favors Hmppt-1 in the tautomerism. According to our calculation, the absence of the ν_{SH} peaks around 2437−2553 cm^{-1} in the experiment also disfavors the existence of Hmppt-2 in the sample.

The GIAO results of the ^{13}C and ^{1}H NMR chemical shifts of all tautomers are compared with the experimental data in Tables 5−8. Because the CSGT results are basically consistent with the GIAO results, we have collected the CSGT results in Tables 5S−8S of the Supporting Information. From the average errors of the calculations, we found that the ^{13}C NMR chemical shifts of Hmppt-1 match better with the experimental data than do those of Hmppt-2, and the same is true for those of Hmppt-d-1 and Hmppt-d-2. These results support the conclusion that Hmppt-1 and Hmppt-d-1 are favored in solution, specifically in DMSO. From the calculated ^{1}H NMR results, we can see that Hmppt has an active H (from N−H) with the chemical shift ranging from 9.2 to 10.7 ppm. For Hmppt-2, we found that the chemical shift for H (from S−H) ranges from 4.8 to 5.3 ppm. The experimental value is 12.84 ppm, much closer to the theoretical prediction of Hmppt-1. This fact thus strongly suggests that the Hmppt-1 form is favored. The solvent effects for the NMR properties of both tautomers were not considerable, since the average errors of the chemical shifts predicted in the gas and solution phases are roughly the same. In addition, for different levels of theory (ab initio and DFT) and methods computing NMR parameters (GIAO and CSGT), there are no significant differences in the results.

Similarly, the calculated ^{13}C NMR chemical shifts also indicate that Hmppt-d-1 is favored (see Tables 7 and 8). Moreover, we notice that the theoretical chemical shifts for the active H (from O−H) in Hmppt-d-1 and for the active H (from N−H) in Hmppt-d-2 are 6.9−7.4 and 10.5−12.2 ppm, respectively, whereas the experimental value is about 9.8 ppm, roughly between these two ranges. This indicates that both tautomeric forms contribute to the NMR spectrum of Hmppt dimer and that Hmppt-d-1 is only slightly more favored than Hmppt-d-2.

UV−vis absorption spectra of Hmppts and its dimers calculated with TDDFT on different levels are compared with the available experimental data in Table 9. For Hmppt-1 and Hmppt-2, we found that calculations with the large basis set, 6-311++G(2df,p), give better results than do those with the small basis set, 6-31G(d,p), but they show the same tendency. So, results of the monomers from the small basis set are shown only in the Supporting Information for comparison. Because of the sizes of the dimers, our computational resources only permitted us to carry out calculations based on the small basis set. Calculations of the monomers suggest that such small basis set results are still acceptable as a compromise between performance and accuracy. As different density functionals are concerned, we found that PBEPBE gives similar results as B3LYP does, so we only list the B3LYP results in Table 9 and keep the PBEPBE results in the Supporting Information for reference.

The maximum UV−vis absorption wavelength, λ_{max}, of Hmppt was determined experimentally to be 326 nm. Calculations for Hmppt-1 yield a relatively accurate estimation of these absorption peak positions (see Table 9), whereas calculations for Hmppt-2 do not support the existence of such a peak in the proximity of 326 nm. This strongly disfavors Hmppt-2 in the tautomerism. We can also reach a similar conclusion for Hmppt dimers. Our theoretical prediction (246 nm) matches the experimental λ_{max} value 238 nm well for Hmppt-d-1, while Hmppt-d-2 has only very weak peaks around 238 nm (at 234 nm), which certainly cannot be considered as candidates for $\lambda_{max.}$ On the other hand, Hmppt-d-2 does show very strong peaks above 400 nm in our calculations (444 nm, not shown in Table 9), which were not observed in our previous experiments. Comparison of the calculations in the gas phase and in H_2O shows that the solvation effects are negligible. Hence, the characteristics of the corresponding UV−vis spectra strongly infer that the structure of Hmppt-d-1 represents the actual structure better than does Hmppt-d-2.

Conclusions

We have presented here a comprehensive theoretical study on the tautomers of Hmppt and its dimer in the vacuum and in polar solutions (DMSO and H_2O). Comparisons were also made with Hdppt and its dimeric form to substantiate our conclusions about the dominant tautomeric form observed in our previous experiments. Calculations at a range of levels of theory consistently support a preference for the thione form, although the degrees of the preferences may vary. This study can be used as a reference for investigating other similar molecules.

Acknowledgment. Financial support from the Natural Sciences and Engineering Research Council (NSERC) of Canada, Canadian Institutes of Health Research (CIHR), and Canada Foundation for Innovation (CFI) is gratefully acknowledged. WestGrid and C-HORSE (CFI) have provided us the necessary computational resources. Y.A.Z. would like to thank Prof. Wei Quan Tian of Jilin University and Dr. Wei (David) Deng of Gaussian Inc. for help with some of the calculations.

Supporting Information Available: Additional tables and figures as noted in the text. This material is available free of charge via the Internet at http://pubs.acs.org.

References and Notes

(1) Metzner, P.; Hogg, D. R.; Walter, W.; Voss, J. In *Organic Compounds of Sulphur, Selenium and Tellurium*; Hogg, D. R., Ed.; The Chemical Society: London, 1977; Vol. 4, p 125; and 1979; Vol. 5, p 118.

(2) (a) Block, E. *Reactions of Organosulfur Compounds*; Academic: New York, 1978; p 26. (b) Cremlyn, R. J. *An Introduction to Organosulfur Chemistry*; Wiley: New York, 1996; Chapters 10 and 11.

(3) Maw, G. A. In *Sulfur in Organic and Inorganic Chemistry*; Senning, A., Ed.; Marcel Dekker: New York 1972; Vol. 2, p 113.

(4) Steliou, K.; Mrani, M. *J. Am. Chem. Soc.* **1982**, *104*, 3104 and references therein.

(5) (a) Monga, V.; Patrick, B. O.; Orvig, C. *Inorg. Chem.* **2005**, *44*, 2666. (b) Monga, V.; Thompson, K. H.; Yuen, V. G.; Sharma, V.; Patrick, B. O.; McNeill, J. H.; Orvig, C. *Inorg. Chem.* **2005**, *44*, 2678.

(6) Lewis, J. A.; Puerta, D. T.; Cohen, S. M. *Inorg. Chem.* **2003**, *42*, 7455.

(7) Tilbrook, G.; Hider, R.; Moridani, M. Patent WO 98/25905, 1998.

(8) Hoyoku, N.; Yukihiro, K.; Toshihiko, S.; Susumu, Y.; Hiromichi, M.; Yoichi, I. U.S. Patent 5093505, 1992.

(9) Albert, A. *Heterocyclic Chemistry an Introduction*; Athlone: London, 1959; p 424.

(10) Stoyanov, S.; Petkov, I.; Antonov, L.; Stoyanova, T. *Can. J. Chem.* **1990**, *68*, 1482.

(11) Besso, H.; Imafuku, K.; Matsumura, H. *Bull. Chem. Soc. Jpn.* **1977**, *50*, 3295 and references therein.

(12) Roberts, J. D.; Caserio, M. C. *Basic Principles of Organic Chemistry*; W. A. Benjamin: New York, 1964; p 744.

(13) (a) Becke, A. D. *Phys. Rev. A* **1988**, *38*, 3098. (b) Lee, C.; Yang, W.; Parr, R. G. *Phys. Rev. B* **1988**, *37*, 785.

(14) Weinhold, F. Natural Bond Orbital Methods. In *Encyclopedia of Computational Chemistry*, Schleyer, P. V. R., Allinger, N. L., Clark, T., Gasteiger, J., Kollman, P. A., Schaefer, H. F., III, Schreiner, P. R., Eds.; Wiley: Chichester, UK, 1998; Vol. 3, pp 1792−1811.

(15) (a) London, F. *J. Phys. Radium.* **1937**, *8*, 3974. (b) McWeeny, R. *Phys. Rev.* **1962**, *126*, 1028. (c) Ditchfield, R. *Mol. Phys.* **1974**, *27*, 789. (d) Dodds, J. L.; McWeeny, R.; Sadlej, A. J. *Mol. Phys.* **1980**, *41*, 1419. (e) Wolinski, K.; Hilton, J. F.; Pulay, P. *J. Am. Chem. Soc.* **1990**, *112*, 8251.

(16) (a) Keith, T. A.; Bader, R. F. W. *Chem. Phys. Lett.* **1992**, *194*, 1. (b) Keith, T. A.; Bader, R. F. W. *Chem. Phys. Lett.* **1993**, *210*, 223. (c)

Cheeseman, J. R.; Frisch, M. J.; Trucks, G. W.; Keith, T. A. *J. Chem. Phys.* **1996**, *104*, 5497.

(17) (a) Cancès, M. T.; Mennucci, B.; Tomasi, J. *J. Chem. Phys.* **1997**, *107*, 3032. (b) Cossi, M.; Barone, V.; Mennucci, B.; Tomasi, J. *Chem. Phys. Lett.* **1998**, *286*, 253. (c) Mennucci, B.; Tomasi, J. *J. Chem. Phys.* **1997**, *106*, 5151.

(18) Scott, A. P.; Radom, L. *J. Phys. Chem.* **1996**, *100*, 16502.

(19) (a) Runge, E.; Gross, E. K. U. *Phys. Rev. Lett.* **1984**, *52*, 997. (b) Gross, E. K. U.; Kohn, W. *Phys. Rev. Lett.* **1985**, *55*, 2850.

(20) (a) Perdew, J. P.; Burke, K.; Ernzerhof, M. *Phys. Rev. Lett.* **1996**, *77*, 3865. (b) Perdew, J. P.; Burke, K.; Ernzerhof, M. *Phys. Rev. Lett.* **1997**, *78*, 1396.

(21) Frisch M. J.; et al. *Gaussian 03*, Revision C.02, Gaussian, Inc.: Wallingford, CT, 2004.